Title
CT of rib lesions.

Journal
American Journal of Roentgenology, 193(1)

ISSN
0361-803X

Authors
Levine, Benjamin D
Motamedi, Kambiz
Chow, Kira
et al.

Publication Date
2009-07-01

DOI
10.2214/ajr.08.1216

Peer reviewed

Residents
inRadiology

CT of Rib Lesions

Benjamin D. Levine[1]
Kambiz Motamedi
Kira Chow
Richard H. Gold
Leanne L. Seeger

OBJECTIVE. This article discusses how ribs are involved in a variety of traumatic, metabolic, inflammatory, neoplastic, and congenital disorders.

CONCLUSION. We review the normal anatomy pertinent to rib imaging and illustrate the key features of a variety of rib lesions, emphasizing the diagnostic value of CT.

Normal Anatomy

The thorax contains 12 pairs of ribs, 12 thoracic vertebrae, and the sternum. The ribs articulate posteriorly with the vertebral column [1]. Anteriorly, the costal cartilages of the first ribs attach directly to the manubrium by synchondroses, the second through seventh ribs articulate with the manubrium or body of the sternum by synovial cavities, and the eighth through 10th ribs form a synchondrosis with the seventh costal cartilage. The 11th and 12th ribs are often referred to as floating ribs because they end blindly in the anterior abdominal wall [2].

At either side of the suprasternal notch is the sternoclavicular joint, a double diarthrodial (synovial) joint bisected by an articular disk (Fig. 1). A prominent transverse ridge at the manubriosternal joint—the sternal angle or the angle of Louis—forms a palpable landmark for the second costal cartilages and, indirectly, the level of the T4–T5 intervertebral disk [1] (Fig. 2).

The posterior end of each rib is composed of a head, neck, and tubercle. The head articulates with the corresponding vertebra, forming the costovertebral joint. The tubercle, a bony protuberance on the posterior surface of the rib, articulates with the transverse process of the vertebra, forming the costotransverse joint (Fig. 3). The costal groove on the inferomedial aspect of the rib contains the intercostal vessels and nerves.

Teaching Point: Because the costovertebral and costotransverse joints are diarthrodial joints, they are susceptible to the same inflammatory and metabolic disorders that affect other synovium-lined joints.

Teaching Point: On the inferomedial aspect of the rib is the costal groove that contains the intercostal vessels and nerves. Care must be taken to avoid this area when performing interventional procedures.

Calcification of the costal cartilages tends not to be radiographically apparent in most healthy patients younger than 35 years. Before that age, calcification of the costal cartilages may be associated with chronic renal failure, thyroid disease, autoimmune disorders, and chondrosarcoma [2]. The normal patterns of calcification differ between males and females, usually appearing as peripheral parallel lines in males (Fig. 4A) and as central, globular clumps in females (Fig. 4B).

Rib Pathology

Congenital Disorders: Lymphangiomatosis

Lymphangiomatosis is a rare congenital malformation of lymphatic vessels that occupies multiple bones, usually causing osteolysis or, less commonly, sclerosis [3] (Fig. 5).

Neoplastic Disorders

Metastasis—Metastatic disease is the most common malignant rib lesion [4] (Fig. 6). Most often, the primary neoplasm is in the breast, prostate gland, lung, or kidney. Rib metastases may be osteolytic, sclerotic, or mixed. Rib lesions detected on bone scintigraphy often require further characterization with radiography or CT to improve specificity (Fig. 7).

Teaching Point: Metastasis is the most common malignant rib lesion.

Teaching Point: Although bone scintigraphy is highly sensitive for rib lesions, it lacks specificity. Correlative radiography or CT improves specificity.

Keywords: CT; diagnostic imaging; ribs, abnormalities; ribs, neoplasms; scintigraphy, ribs; thorax

DOI:10.2214/AJR.08.1216

Received May 9, 2008; accepted after revision August 4, 2008.

[1]All authors: Department of Radiology, David Geffen School of Medicine at UCLA, 200 UCLA Medical Plaza, Ste. 165-57, Los Angeles, CA 90095-6952. Address correspondence to L. L. Seeger (lseeger@mednet.ucla.edu).

AJR 2009; 193:5–13

0361–803X/09/1931–5

Pancoast tumor—The most common cause of a Pancoast tumor is an apical lung carcinoma that invades the chest wall. The tumor may involve the brachial plexus, cervical sympathetic ganglia, and superior mediastinum [5] (Fig. 8).

Gorham disease—Gorham disease (also known as vanishing bone disease, hemangiomatosis of bone, or massive osteolysis) is characterized by extensive and progressive osteolysis of contiguous bones [6] (Fig. 9).

Chondrosarcoma—Chondrosarcoma, the most common primary malignant rib neoplasm, usually arises at or near the costochondral junction [7]. Its incidence tends to peak at the age of 50 years; it is rare in individuals younger than 20 years. Although some chondrosarcomas may not have radiographically visible calcifications, most feature lobulated masses containing the typical flocculent, stippled, or ring- and arclike calcifications (Fig. 10).

Teaching Point: Chondrosarcoma is the most common primary malignant rib lesion, usually occurring at or near the costochondral junction.

Enchondroma—Three percent of enchondromas occur in the ribs. They usually appear as focally expansile, radiolucent lesions that consist pathologically of hyaline cartilage lobules in the medullary cavity (Fig. 11).

Multiple hereditary exostoses—Fifty percent of patients with multiple hereditary exostoses (osteochondromatosis), an autosomal dominant disorder, have lesions in the ribs [3] (Fig. 12). Complications include fractures, pneumothorax, vascular or neural compression, and malignant transformation to chondrosarcoma.

Desmoid tumor—Desmoid tumors are fibroblastic tumors of the musculature that originate in the chest wall in 10–28% of patients [7]. On CT, desmoid tumors appear as homogeneous, nonenhancing soft-tissue masses that may erode adjacent bones and stimulate the formation of periosteal new bone (Fig. 13).

Lymphoma—Diffuse large B-cell lymphoma is the most common type of lymphoma to involve the chest wall and ribs (Fig. 14). It often appears as a large extraosseous soft-tissue mass, with relative preservation of the underlying bony cortex. When it occurs in association with AIDS, lymphoma may cause bone erosion and osteolysis [5].

Fibrous dysplasia—Fibrous dysplasia is the most common benign rib lesion [3]. On CT, it typically shows bony expansion and, often, a ground-glass matrix [3]. It shows increased radiotracer uptake on bone scintigraphy (Fig. 15).

Teaching Point: Fibrous dysplasia, the most common benign rib lesion, shows bony expansion, a ground-glass matrix, and increased tracer uptake on bone scintigraphy.

Aneurysmal bone cyst—An aneurysmal bone cyst is a rapidly growing benign lesion consisting of multiple thin-walled blood-filled cavities [8]. On CT, it is expansile, osteolytic, and eccentrically located (Fig. 16). An aneurysmal bone cyst may also contain fluid levels.

Traumatic Disorders: Acute Rib Fracture

Fractures are the most common lesions to affect the ribs overall [9]. Acute rib fractures may be radiographically occult and even subtle on CT. Fatigue-type stress fractures in the ribs may be associated with sporting activities such as rowing, golf, or other activities that cause repetitive stress [9]. Insufficiency-type stress fractures may be found in association with chronic osteopenia or osteomalacia. Bone scintigraphy has a high negative predictive value for stress fractures (Fig. 17).

Teaching Point: Although acute fractures of normal ribs are common, stress fractures may also occur in the ribs.

Infection: Septic Arthritis

Septic arthritis is most often due to hematogenous spread of *Staphylococcus aureus* originating from a skin lesion. In adults, the sternoclavicular and sacroiliac joints, symphysis pubis, and spine are most frequently affected [10]. Infection may also involve the ribs in places such as the costosternal junction (Fig. 18). CT findings may include soft-tissue edema, articular erosion, joint effusion, subchondral bone destruction, and reactive sclerosis.

Metabolic Disorders

Paget Disease

Paget disease is a disorder of increased bone resorption and formation in older persons that leads to thickening and fragility of the affected bones. It involves, in decreasing order of frequency, the pelvis, femur, skull, tibia, vertebrae, clavicle, humerus, and, in 1–4% of cases, the ribs (Fig. 19).

Teaching Point: Complications of Paget disease include fracture, degenerative joint disease, neurologic compromise, and sarcomatous degeneration.

Gout

Gouty arthritis most frequently affects the foot, hand, wrist, elbow, knee, ankle, and, less frequently, the sacroiliac and sternoclavicular joints [11]. The ribs are infrequently involved. However, an increased incidence in transplant recipients, especially those receiving heart transplants, has been reported [12] (Fig. 20).

Noninfectious Inflammatory Disorders: Ankylosing Spondylitis

Ankylosing spondylitis is a chronic inflammatory arthritis that involves predominantly the sacroiliac, apophyseal, diskovertebral, costovertebral, and costotransverse articulations [13]. Early changes in the costovertebral and costotransverse joints include indistinctness of the subchondral bone, and, in the costovertebral joint, sclerosis that is most evident on the vertebral side [13, 14] (Fig. 21). The changes ultimately progress to bony ankylosis.

Conclusion

The ribs are involved in a variety of traumatic, metabolic, inflammatory, neoplastic, and congenital disorders. CT is useful to further characterize a rib lesion found on radiography or bone scintigraphy. A rib lesion inadvertently discovered on a CT examination of the chest may be the first sign of a systemic disorder or a remote primary neoplasm.

Teaching Point: An understanding of rib anatomy and recognition of CT features of rib pathology facilitates appropriate diagnosis and management.

References

1. Bryan GJ, Davies ER. *Skeletal anatomy*, 3rd ed. New York, NY: Churchill Livingstone, 1996
2. Ontell FK, Moore EH, Shepard JO, Shelton DK. The costal cartilages in health and disease. *RadioGraphics* 1997; 17:571–577
3. Glass RB, Norton KI, Mitre SA, Kang E. Pediatric ribs: a spectrum of abnormalities. *RadioGraphics* 2002; 22:87–104
4. Guttentag AR, Salwen JK. Keep your eyes on the ribs: the spectrum of normal variants and diseases that involve the ribs. *RadioGraphics* 1999; 19: 1125–1142
5. Kuhlman JE, Bouchardy L, Fishman EK, Zerhouni EA. CT and MR imaging evaluation of chest wall disorders. *RadioGraphics* 1994; 14: 571–595
6. Collins J. Gorham syndrome. *Radiology* 2006; 238:1066–1069
7. Tateishi U, Gladish GW, Kusumoto M, et al. Chest wall tumors: radiologic findings and pathologic correlation. Part 2. Malignant tumors. *Radio-*

Graphics 2003; 23:1491–1508

8. Tateishi U, Gladish GW, Kusumoto M, et al. Chest wall tumors: radiologic findings and pathologic correlation. Part 1. Benign tumors. *RadioGraphics* 2003; 23:1477–1490
9. De Maeseneer M, De Mey J, Lenchik L, Evararert H, Osteaux M. Helical CT of rib lesions: a pattern-based approach. *AJR* 2004; 182:173–179
10. Jeung MY, Gangi A, Gasser B, et al. Imaging of chest wall disorders. *RadioGraphics* 1999; 19: 617–637
11. Resnick D. Gouty arthritis. In: Resnick D, ed. *Diagnosis of bone and joint disorders*, 4th ed. Philadelphia, PA: Saunders, 2002:1519–1559
12. Chang PC, Seeger LL, Motamedi K, Chan JB. Tophaceous gout of the first costochondral junction in a heart transplant patient. *Skeletal Radiol* 2006; 35:684–686
13. Resnick D. Ankylosing spondylitis. In: Resnick D, ed. *Diagnosis of bone and joint disorders*, 4th ed. Philadelphia, PA: Saunders, 2002:1023–1081
14. Pascual E, Castellano JA, López E. Costovertebral joint changes in ankylosing spondylitis with thoracic pain. *Rheumatology* 1992; 31:413–415

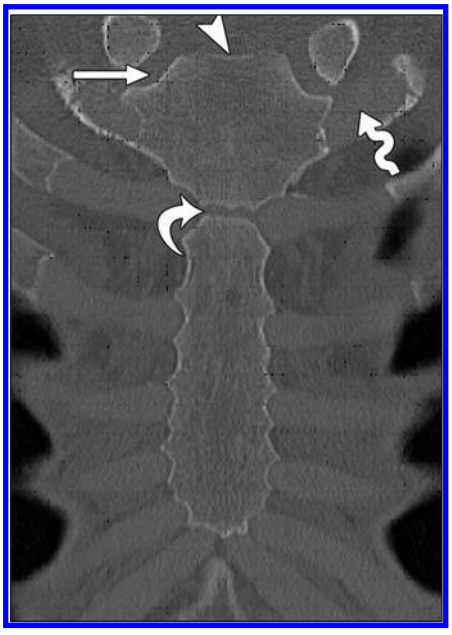

Fig. 1—Coronal reconstructed CT image in normal young woman shows normal sternal manubrium and body with attachments for superior seven costal cartilages. Sternoclavicular joints (*straight arrow*) are at either side of suprasternal notch (*arrowhead*). Note calcified costal cartilage of first rib (*squiggly arrow*) and manubriosternal joint (*curved arrow*).

Fig. 2—Sagittal reconstructed CT image in normal young woman shows prominent transverse ridge at manubriosternal joint, known as sternal angle or angle of Louis (*arrow*).

Fig. 3—Axial CT image with bone window setting in normal young woman shows head of rib articulating with vertebra, forming costovertebral joint (*arrow*). Tubercle, bony protuberance along posterior surface of rib articulates with transverse process, forming costotransverse joint (*arrowhead*). Both are synovial joints.

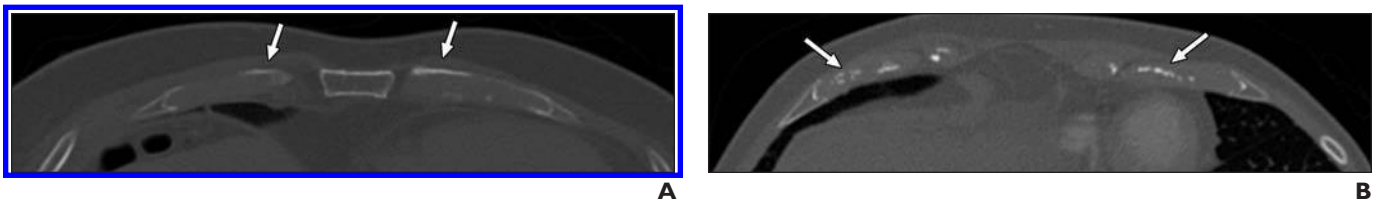

Fig. 4—Costal cartilage calcification patterns.
A, Peripheral, linear calcifications (*arrows*) in 65-year-old man are consistent with male costal cartilage calcification pattern.
B, Central, thick calcifications (*arrows*) in 62-year-old woman are consistent with female costal cartilage calcification pattern.

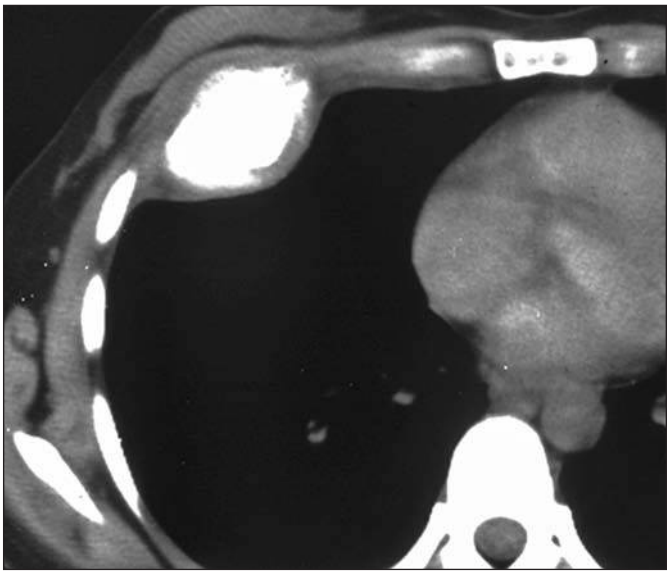

Fig. 5—34-year-old man with lymphangiomatosis of ribs, skull, and femur. Axial CT scan shows expansion and sclerosis of anterior part of rib. Bone scintigraphy (not shown) showed increased tracer uptake at this site.

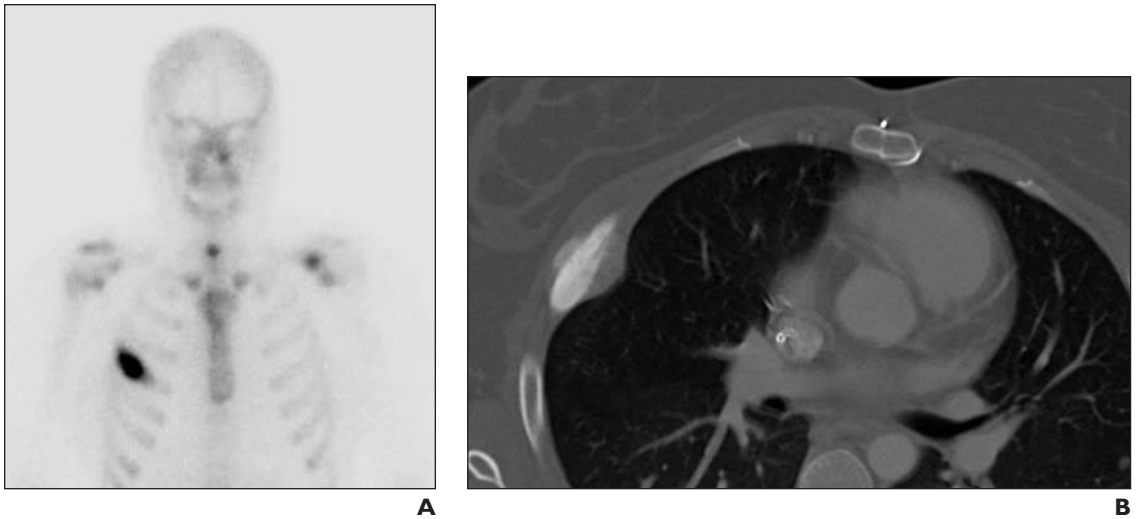

Fig. 6—Rib metastasis from adrenocortical carcinoma in 29-year-old woman.
A and **B,** Bone scintigraphy image (**A**) shows increased radiotracer uptake in right fourth rib corresponding to CT findings (**B**) of sclerotic, expansile process invading adjacent soft tissue.

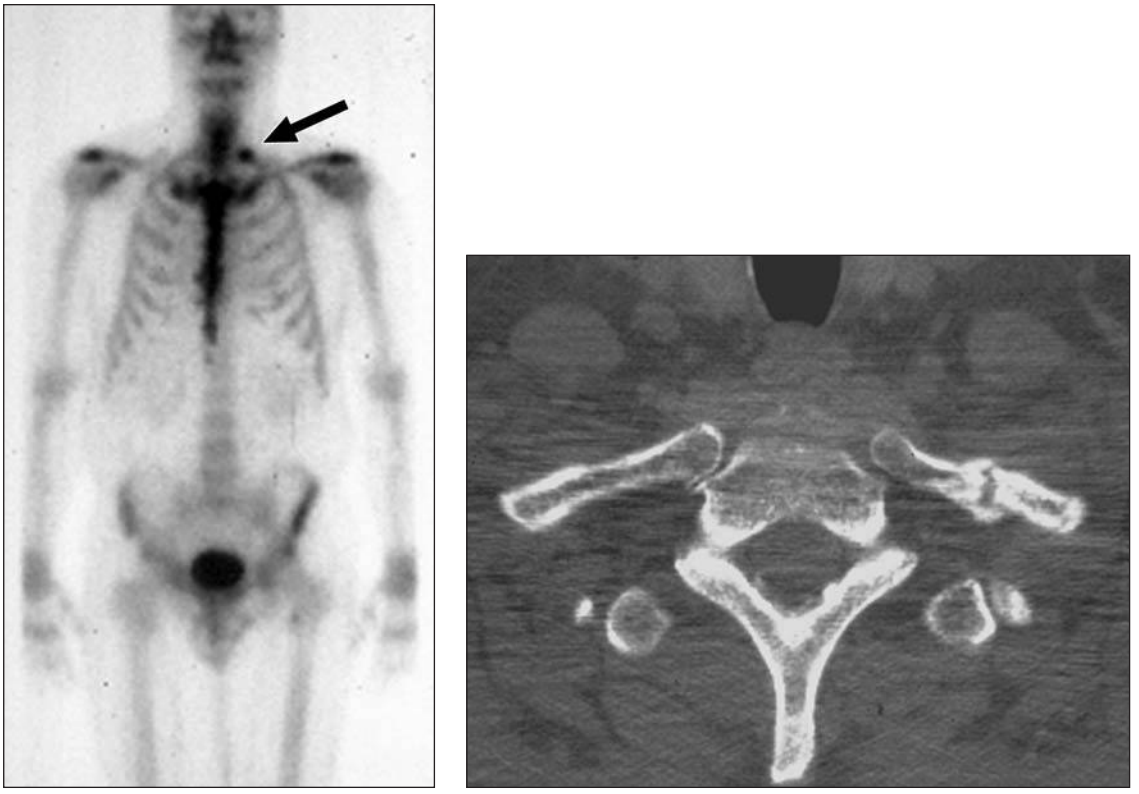

A B

Fig. 7—51-year-old man with melanoma.
A, Bone scintigraphy shows abnormal tracer uptake in left first rib, near costovertebral junction (*arrow*), that is highly suspicious for metastasis. Radiography was negative.
B, CT scan shows fracture of posterior aspect of left first rib, with smooth sclerotic margins of reactive bone indicating nonunion, and no evidence of metastasis.

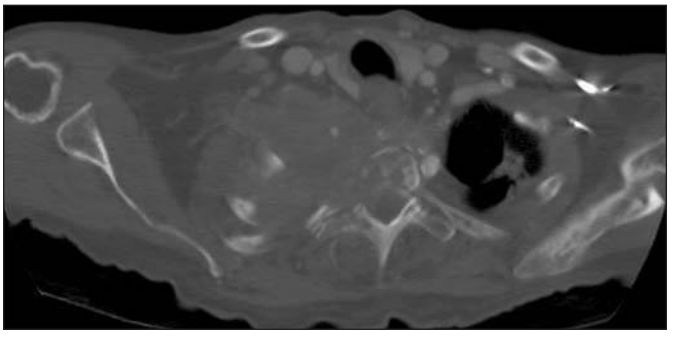

Fig. 8—Pancoast tumor in 67-year-old man. Axial CT scan through lung apices shows large soft-tissue mass in right lung apex and invasion of chest wall and superior mediastinum. The first, second, and third ribs and right side of vertebral body of T3 are partially destroyed.

Fig. 9—Gorham disease in 49-year-old woman with right shoulder pain. CT scan shows complete osteolysis of upper ribs on right. Patient subsequently developed chylous pleural effusion, a known complication of syndrome.

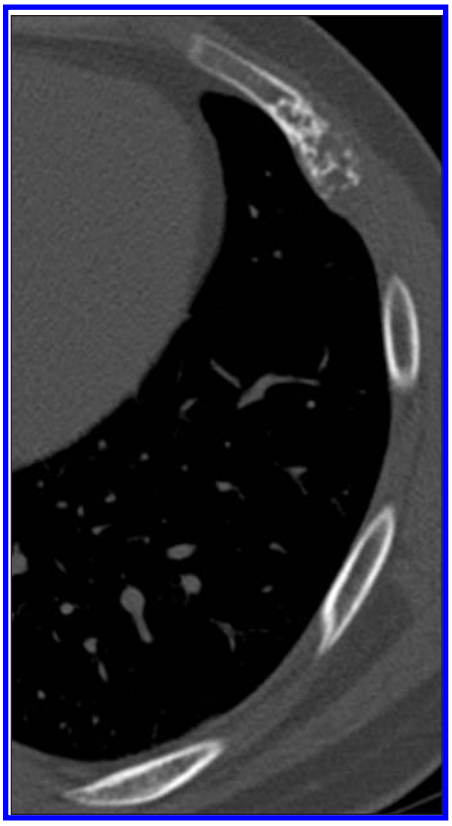

Fig. 10—Low-grade chondrosarcoma in 29-year-old man. Axial CT scan shows mildly expansile lesion of anterior part of left fifth rib. Typical features of cartilage calcification are shown here by stippled ring and arc type pattern.

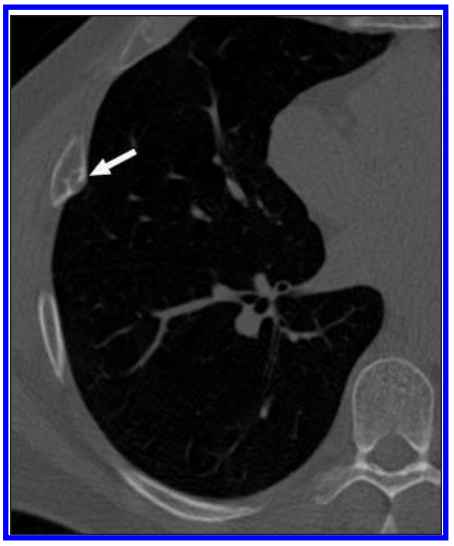

Fig. 11—Enchondroma in 60-year-old man. Axial CT scan shows well-circumscribed focus of radiolucency in lateral aspect of rib and mild focal expansion (*arrow*). Absence of cortical breakthrough or thickening, endosteal scalloping, and periosteal reaction suggests benignancy.

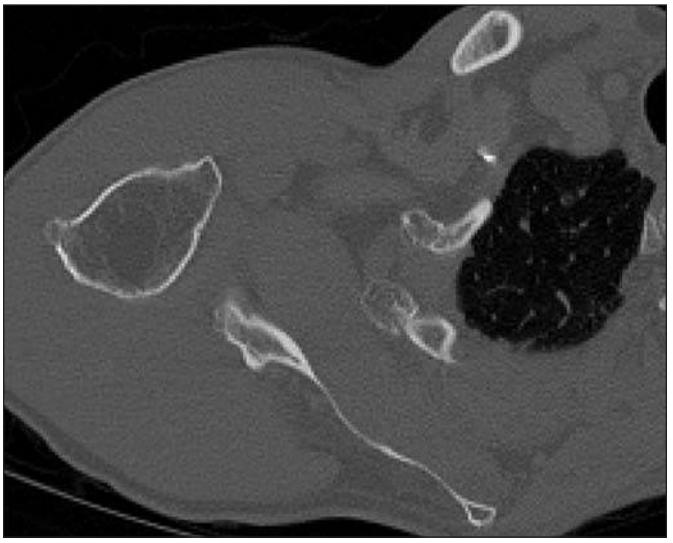

Fig. 12—Multiple hereditary exostoses in 34-year-old man with enlarging, painful right shoulder mass. Axial CT scan shows multiple exostoses arising from ribs, scapula, and humerus.

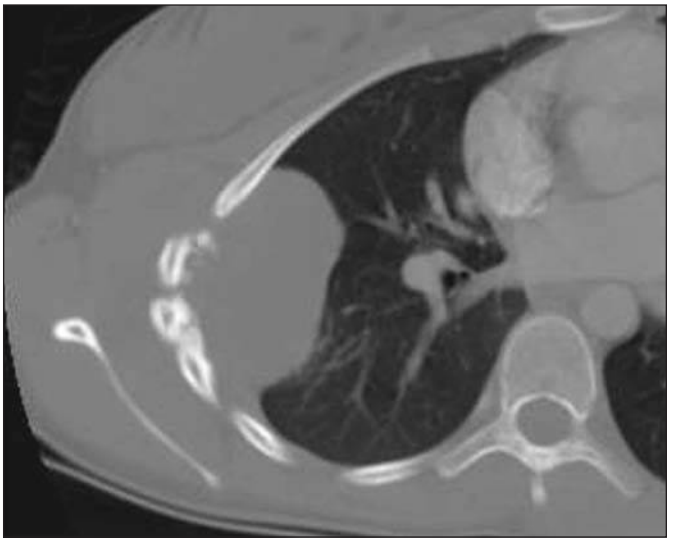

Fig. 13—14-year-old girl with desmoid tumor. Axial CT scan shows soft-tissue mass surrounding right third through seventh ribs in right lateral chest wall. Ribs exhibit exuberant periosteal new bone.

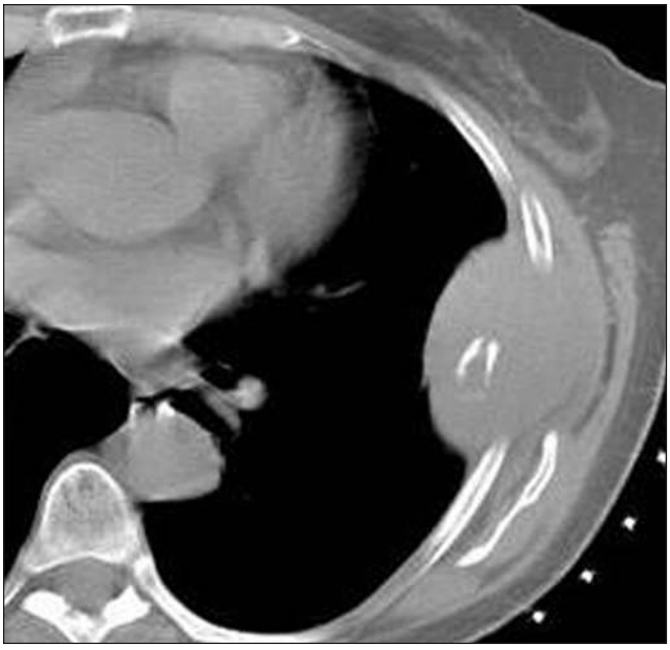

Fig. 14—53-year-old woman with large B-cell lymphoma. Axial CT scan shows large soft-tissue mass involving left sixth rib.

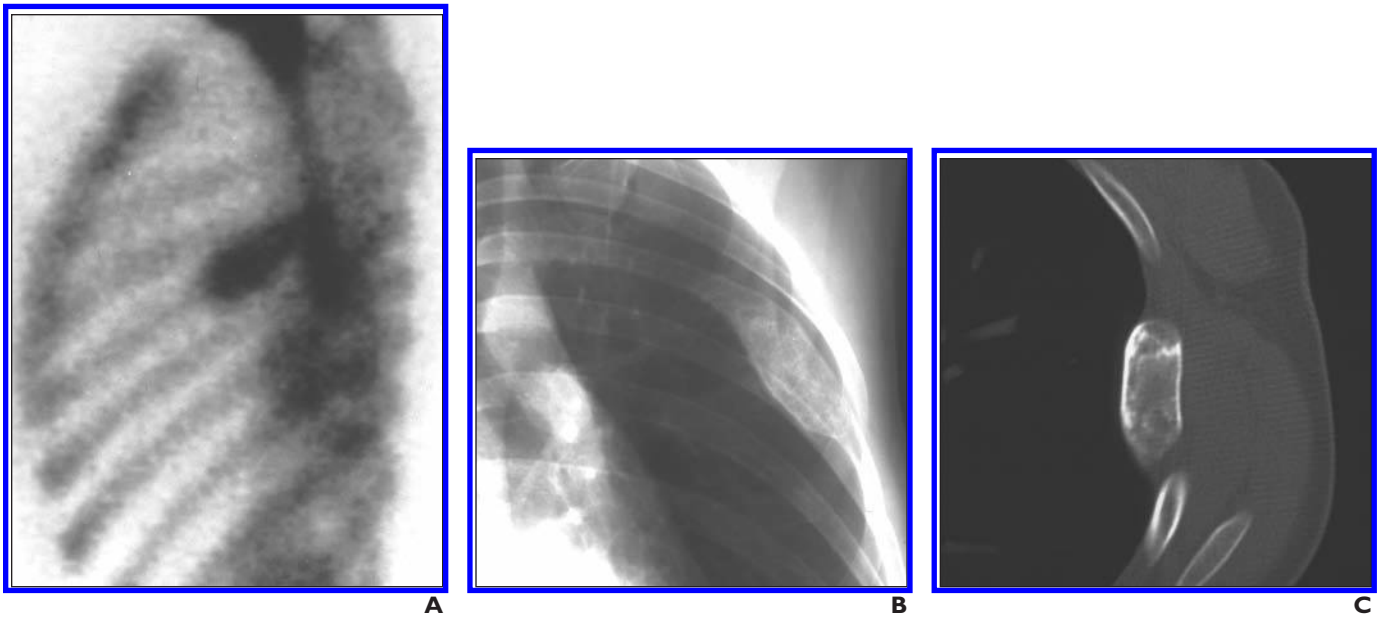

Fig. 15—30-year-old woman with fibrous dysplasia.
A–C, Focus of increased radiotracer uptake on bone scintigraphy **(A)** corresponds to chest radiographic (**B**) and axial CT (**C**) findings of expansile lesion of left fifth rib with ground-glass appearance.

Fig. 16—39-year-old man with aneurysmal bone cyst. Axial CT scan shows expansile osteolytic lesion with soft-tissue extension and thin internal trabeculations.

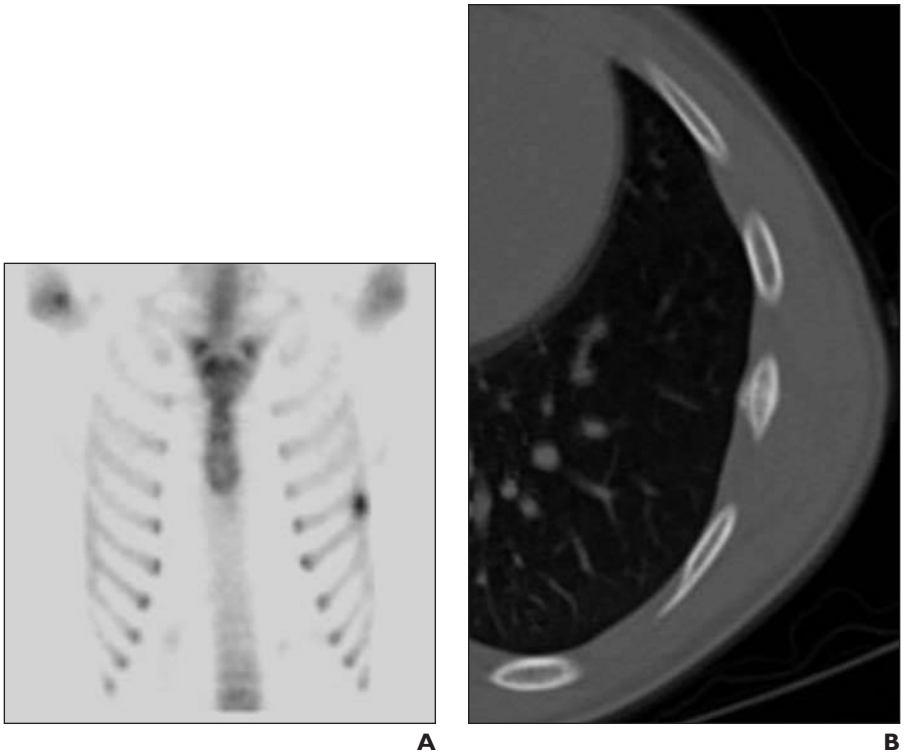

A **B**

Fig. 17—Fatigue-type stress fracture in 20-year-old female athlete with left rib pain. Radiographs of ribs were negative.
A, Subsequent bone scintigraphy reveals abnormal radiotracer uptake in lateral aspect of left seventh rib.
B, Axial CT scan shows fluffy periosteal reaction and mild sclerosis, corresponding to area of abnormal uptake on bone scan.

Fig. 18—51-year-old man with acute myelogenous leukemia and hepatitis C who presented with focal pain. Axial CT scan shows destruction at junction of left first costal cartilage and manubrium with surrounding soft-tissue edema. Aspiration revealed *Pseudomonas aeruginosa*.

Fig. 19—81-year-old man with Paget disease. Axial CT scan shows increased density, enlargement, and cortical thickening of posteromedial aspect of left ninth rib and secondary degenerative arthritis of costovertebral and costotransverse articulations. Abnormal radiotracer uptake at corresponding site was seen on bone scintigraphy.

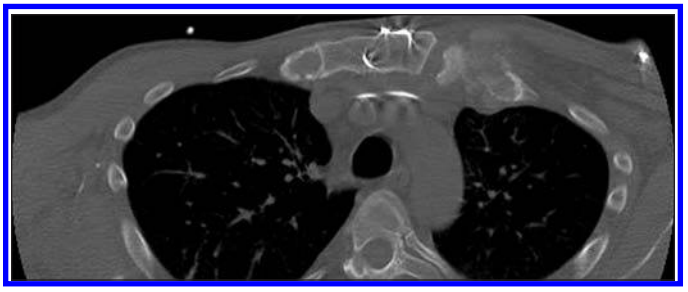

Fig. 20—Tophaceous gout in 50-year-old man who underwent recent orthotopic heart transplantation, and who presented with fever and chest pain. Axial CT scan shows soft-tissue mass at left first costochondral junction, in association with rib destruction and amorphous increased soft-tissue density.

Fig. 21—Ankylosing spondylitis in 42-year-old woman. Axial CT scan shows subchondral erosions, irregularity, and sclerosis of both costovertebral joints that is more pronounced on vertebral side of joints. Note erosion and reactive sclerosis along anterior surface of vertebral body (Romanus lesion).

This article has been cited by:

1. Patrick Hoffstetter, Christian Dornia, Stephan Schäfer, Merle Wagner, Lena M Dendl, Christian Stroszczynski, Andreas G Schreyer. 2014. Diagnostic significance of rib series in minor thorax trauma compared to plain chest film and computed tomography. *Journal of Trauma Management & Outcomes* **8**, 10. [CrossRef]
2. Hiroshi Kaneko, Hiroshi Kitoh, Akiyoshi Mabuchi, Kenichi Mishima, Masaki Matsushita, Naoki Ishiguro. 2012. Isolated bifid rib: Clinical and radiological findings in children. *Pediatrics International* **54**:10.1111/ped.2012.54.issue-6, 820-823. [CrossRef]